1-2021

Microstructural and Chemical Characterization of a Purple Pigment from a Faiyum Mummy Portrait

Glenn Gates
Walters Art Museum

Yaqiao Wu
Boise State University

Jatuporn Burns
Idaho National Laboratory

Jennifer Watkins
Boise State University

Darryl P. Butt
University of Utah

Received: 18 August 2020 | Accepted: 15 September 2020

DOI: 10.1002/ces2.10075

ORIGINAL ARTICLE

International Journal of Ceramic Engineering & Science

Microstructural and chemical characterization of a purple pigment from a Faiyum mummy portrait

Glenn Gates[1] | **Yaqiao Wu**[2,3] | **Jatuporn Burns**[4] | **Jennifer Watkins**[2,4] | **Darryl P. Butt**[5]

[1]Department of Conservation, Collections and Technical Research, Walters Art Museum, Baltimore, Maryland, USA

[2]Department of Materials Science and Engineering, Boise State University, Boise, Idaho, USA

[3]Center for Advanced Energy Studies, Idaho Falls, Idaho, USA

[4]Idaho National Laboratory, Idaho Falls, Idaho, USA

[5]College of Mines and Earth Sciences, University of Utah, Salt Lake City, Utah, USA

Correspondence
Glenn Gates, Department of Conservation, Collections and Technical Research, Walters Art Museum, 600 N. Charles Street, Baltimore, MD 21201, USA.
Email: ggates@thewalters.org

Abstract

Results are presented from analyses that were conducted to explain the presence of chromium, detected noninvasively using energy-dispersive X-ray fluorescence (XRF), in the unusually large (2-3mm diameter) rough gem-like purple pigment particles in the paint used for a Faiyum mummy portrait. An approximately 50 μm diameter particle of the chromium-containing purple pigment was extracted from the *Portrait of a Bearded Man*, dated to Roman Imperial Egypt in the second century, *circa* 170-180 CE, accession #32.6 in the Walters Art Museum collection. The particle was characterized using energy-dispersive X-ray fluorescence analysis, electron microscopy, diffraction, and atom probe tomography. It is demonstrated that the purple pigment particle is a heterogeneous organic pigment, specifically, a lake pigment likely derived from either plant or insect matter, which contains minor percentages of both transition metals and alkali / alkali earth metals, with nanometer-scale crystallites of lead carbonates and sulfates. The analyses revealed for the first time the nanoscale microstructure and stratigraphy in an ancient lake pigment. Results suggest that similarities with respect to time period and place of production may be developed among unprovenienced Faiyum mummy portraits to help localize workshops or artists, using analyses focused on lake pigments to characterize specifically metal-based mordants.

KEYWORDS

lake, pigment, mordant, Faiyum, mummy, portrait, chromium

1 | INTRODUCTION

The earliest known writing referring ancient mummy portraiture is a brief note in the elder Pliny's *Naturalis Historia,* which dates to the first century CE.[1,2] The portraits from Roman Imperial Egypt, such as the example under discussion shown in Figure 1, *Portrait of a Bearded Man*, were intended to reflect not only the age, gender, and likeness of the individual, but the real or aspirational status of the subject of the portrait, both in his or her life on earth and anticipated rebirth in the next world. These funerary portraits were ultimately affixed to the exterior of the mummified individual using wrappings or to the sarcophagus of the deceased.[2-4] The practice of such portraiture is known to date from shortly after Egypt became a Roman province in 30 BCE, into the third century CE.[2]

FIGURE 1 (A) Photograph of the*Portrait of a Bearded Man* (Walters Art Museum #32.6), dated*circa*170-180 CE from Roman Imperial Egypt [40.5 cm by 20 cm]; this "Faiyum" mummy portrait is photographed on the left under visible radiation; on the right in (B) is the portrait under ultraviolet "A" (315-400 nm) radiation. The purple *clavi*on the shoulders appear pink-orange colored under UVA, indicated by an arrow

Although some of these mummy portraits were unearthed as early as the beginning of the 17th century in Sakkara,[5] the majority of these works did not appear on the art market until the late 1880s, and the supply was almost completely exhausted by the early 1920s.[5] Approximately 1100 mummy portraits are now known in collections worldwide. The absence of proper archeological methods used in acquiring and documenting the majority of these portraits has led to a desire to find material-based connections among portraits to help establish similarities or groupings that might perhaps even help to identify their ultimate provenience. To this end, the *Ancient Panel Paintings: Examination Analysis and Research (APPEAR) Project and Database*[6] was initiated in 2013 by Marie Svoboda, Conservator of Antiquities at the J. Paul Getty Museum. The APPEAR Project is a multinational collaboration involving more than forty institutions that are sharing scientific information and analytical results through a publically accessible database pertaining to mummy portraits and their constituent materials, including pigments, paint binders, textiles, mummification residues, and wood species identifications.

The portrait under consideration in this paper, analyzed as a contribution to APPEAR and shown in Figure 1, depicts a bearded man wearing a toga decorated with two purple *clavi*. *Clavi* are the purple stripes on the left and right shoulders of Roman tunics used to indicate individuals of high social stature.[7] The portrait was acquired by Henry Walters from the noteworthy art dealer Dikram Kelekian in 1912 and resides now in the Walters Art Museum, Baltimore, Maryland. Its paint is based on beeswax, a so-called encaustic binder, painted on a thin 40 x 20 x 0.25 cm *Tilia sp* wood panel; approximately 80% of Faiyum portraits are on this wood, commonly called lime or linden.[8]

In the ancient Mediterranean world, purple-dyed clothing was reserved at various times for royalty, individuals of high social status, or affluent individuals.[9] The most valued ancient purple, called Tyrian purple, is a bromine-containing organic dye, extracted from the hypobranchial gland of so-called "murexes" or "rock snails" that are mollusks of the family Muricidae.[10] By the later first and second centuries CE, however, purple was used among all classes throughout the Roman Empire for clothing and other display articles; papyri of Egypt from this time document the open use of purple dye and purple clothing by private persons and slaves.[11] Lower quality of purple dyes and pigments were produced in ancient Egypt to supply demand, and these include various combinations of: plant matter, producing madder, alkanet, and indigo; lichens producing orchil (archil) and folium; insects, producing kermes and lac; and metal mordants to adjust colors of dyes.[12]

Preliminary examination of the *clavi* in the Portrait of a Man at the Walters showed that under ultraviolet radiation the *clavi* fluoresced pink-orange under long-wave ultraviolet radiation (315-400nm), as shown in Figure 1. This observation suggested the presence of an organic lake pigment, that is, a pigment formed by affixing an organic dye onto an inorganic substrate, usually through the use of a metal mordant. Most notably, however, careful micro-stereoscopic examination of the *clavi* revealed the presence of unusually large, rough gem-like purple particles embedded in the purple paint, shown in Figure 2, with some as large as 3 mm diameter. For comparison, large pigment particles in ancient paintings are usually on the order of 20-50 μm. Subsequent nondestructive, air-path, energy-dispersive X-ray fluorescence (XRF) analyses of these purple particles revealed that they contained lead, aluminum, titanium, silicon, potassium, iron, and sulfur with, surprisingly, chromium, estimated at concentrations in the parts-per-thousand range. No bromine was detected during XRF analyses, suggesting that the purple was probably not the valuable Tyrian purple, a colorant containing 6,6'-dibromoindigo,[13] nor was it lichen-based, which would also contain bromine.[14]

With the surprising discovery of chromium in the unusually large, rough gem-like particles embedded in the purple paint used for the *clavi*, several possible explanations were considered:

- Could ground precious or semiprecious stones containing chromium, such as garnet, spinel, or even ruby have been added at the request of the individual portrayed, in an attempt to enhance status in the afterlife? The large particle size, gem-like appearance and the location restricted to the *clavi* might support this.

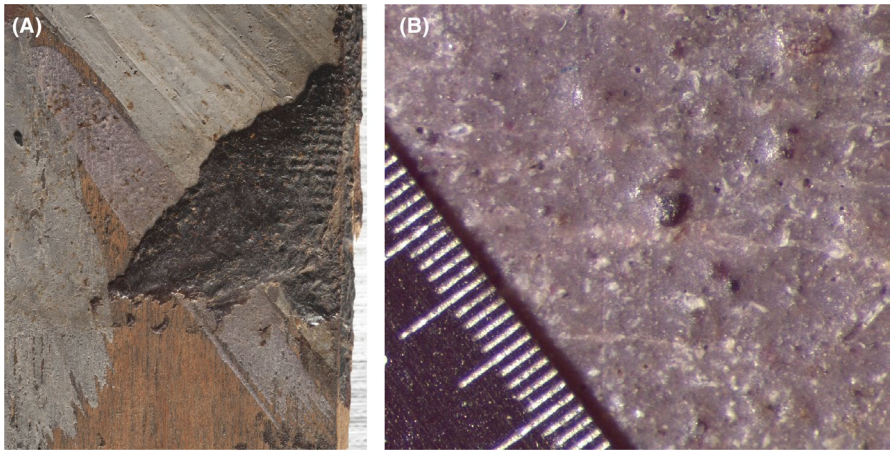

FIGURE 2 (A) On the left is a detail photograph of the faded, proper left purple *clavus*(5 cm long) depicted on the*Portrait of a Bearded Man*; it is partly underneath ancient embalming material that now appears dark brown or black. In (B) on the right is a magnified detail (1 division = 1 mm on the inset ruler) of the same proper left *clavus*, showing at the center of the image, a large purple pigment particle with rough gem-like appearance, among others of smaller size; a visually similar but much smaller particle was extracted from the portrait for analysis

- Could the chromium, along with the aluminum and iron, suggest a preferred or selected ingredient for dyeing in the ancient world, such as an alum mordant containing intentional or fortuitous iron and chromium traces that would yield a superior color?[15-17]
- Given the known concentrations of chromium in Egyptian clays and Nile sediments at around 100-500 ppm,[18] that is, at concentrations similar to that suggested by XRF analyses of the Portrait of a Man, was the detection of chromium relatively insignificant regarding provenience, and perhaps merely indicative of the portrait's production in Egypt?

Therefore, the purple paint was sampled for analysis; the material extracted is presented in Figure 3. The primary purpose of this analytical investigation was to determine a reasonable explanation for the presence of chromium in the purple pigment. Such investigation could provide insight into the source and possible method of synthesis of this colorant, and perhaps, yield data associating the Walters unprovenienced *Portrait of a Man* with other mummy portraits containing comparable materials, establishing similarities concerning place and time of production.

2 | RESULTS AND DISCUSSION

2.1 | SEM and EDS of the purple pigment particle

Thirteen areas on the pigment particle were analyzed by EDS, as shown in Figure 4, with corresponding semi-quantitative EDS analyses summarized in Table 1 as approximate atomic percent (at%). No bromine was detected, confirming the previous XRF results, and suggesting the purple was probably not derived from either mollusks, as Tyrian purple, nor from lichens or algae, as orchil or folium, a.k.a. "false shellfish purples."[19]

In all thirteen EDS analyses, the approximate atomic percent of carbon was the highest of any element detected,

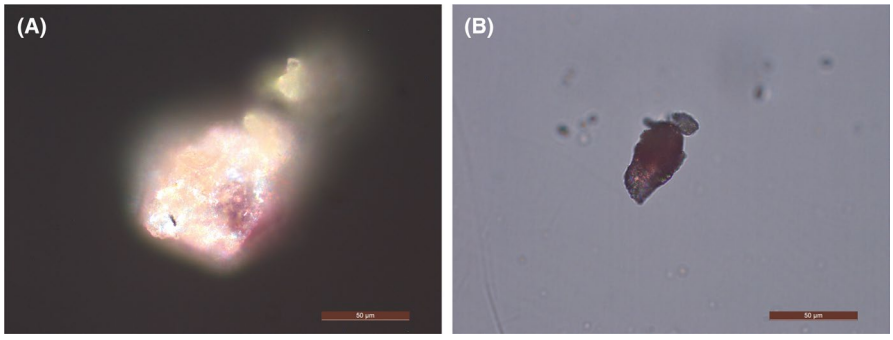

FIGURE 3 (A) On the left is an optical photomicrograph of the material removed from the proper left*clavus*of the *Portrait of a Bearded Man*under dark field illumination; on the right in (B) is the material sent for analysis, after most of the white surrounding material was removed with a scalpel, photographed using transmitted light with partially crossed polarizing filters

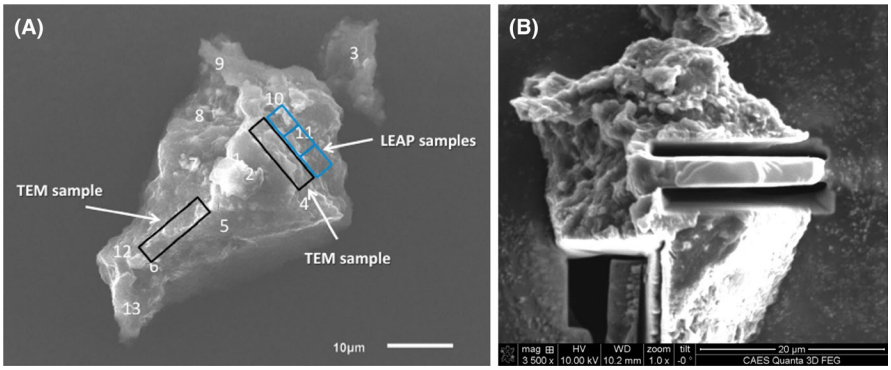

FIGURE 4 (A) On the left is a scanning electron micrograph of the pigment particle showing the locations of thirteen EDS scans, and where TEM (#=2, in black) and LEAP (#=3, in blue) samples were subsequently removed by FIB. The SEM micrograph on the right in (B) is the pigment particle following extraction of the TEM and LEAP samples by FIB milling

TABLE 1 Semi-quantitative chemical analyses (approximate atomic percent) obtained by EDS of thirteen regions on the pigment particle as shown in Figure 4

REGION	Pb	O	C	S	Al	Sl	Mg	P	Cl	K	Cr	Fe	Na	Ca
Spot 1	3.57	6.93	88.78		0.59	0.13								
Spot 2	3.57	6.93	88.78		0.59	0.13								
Spot 3	1.14	11.84	86.55		0.47									
Spot 4	0.18	16.35	77.16	1.3	4.02	0.25	0.09	0.14	0.1	0.24	0.08	0.09		
Spot 5	2.3	10.65	84.04		2.56	0.18			0.1	0.16				
Spot 6	0.74	13.61	76.56	1.79	5.77	0.41	0.17		0.23	0.64	0.04	0.05		
Spot 7	0.79	33.95	58.78	1.11	4.34	0.32	0.22			0.4			0.09	
Spot 8	2.3	10.65	84.04		2.56	0.18			0.1	0.16				
Spot 9	0.74	18.44	78.94		1.67	0.05	0.03			0.08				0.06
Spot 10	0.39	12.15	83.08	0.45	1.96	1.67	0.09	0.05	0.04	0.05			0.03	0.03
Spot 11	0.56	16.57	76.04	1.27	4.62	0.42	0.1			0.32	0.04	0.06		
Spot 12	0.26	16.75	79.45	0.55	2.46	0.16	0.11	0.05		0.16	0.02	0.03		

>75 at %; this is consistent with the particle being primarily organic. Lead, oxygen, and aluminum were also detected in all thirteen EDS analyses, along with low atomic percent silicon (except at site 3). Furthermore, the greatest approximate at% for aluminum corresponds with detection of sulfur and high at% potassium. In fact, Figure 5 does show a reasonably good, positive correlation, $r^2 = .89$, between potassium and aluminum in the EDS results. With the exception of the lead detected by EDS, all these findings suggest the presence of an organic lake pigment, that is, an organic dye affixed to an amorphous hydrated alumina substrate through the use of a potash alum mordant, potassium aluminum sulfate, $KAl(SO_4)_2 \cdot 12H_2O$, used for dying since 1000 BCE.[20] "Alum was the most common mordant in ancient times: the clear kind for delicate tints, and the brownish kind, containing iron salts, for dark dyes."[21] The western desert of Egypt, including the Dakhla and Kharga Oases, was a major ancient source of alum; similar evaporites in the region today include $FeAl_2(SO_4)_4 \cdot 22H_2O$, $MgAl_2(SO_4)_4 \cdot 22H_2O$, $NaAl(SO_4)_2 \cdot 6H_2O$, and $Al2(SO_4)_3 \cdot 17H_2O$.[22]

Much of the lead reported in these EDS data might be attributed to the lead-based white paint surrounding the purple particle, it is a ubiquitous, ancient paint comprised of a mixture of white basic lead (II) carbonate and neutral lead (II) carbonate pigments, for example, the minerals hydrocerussite and cerussite, respectively, bound in a beeswax-based medium. However, subsequent focused ion beam sectioning of the purple pigment revealed a more complex explanation for the lead;

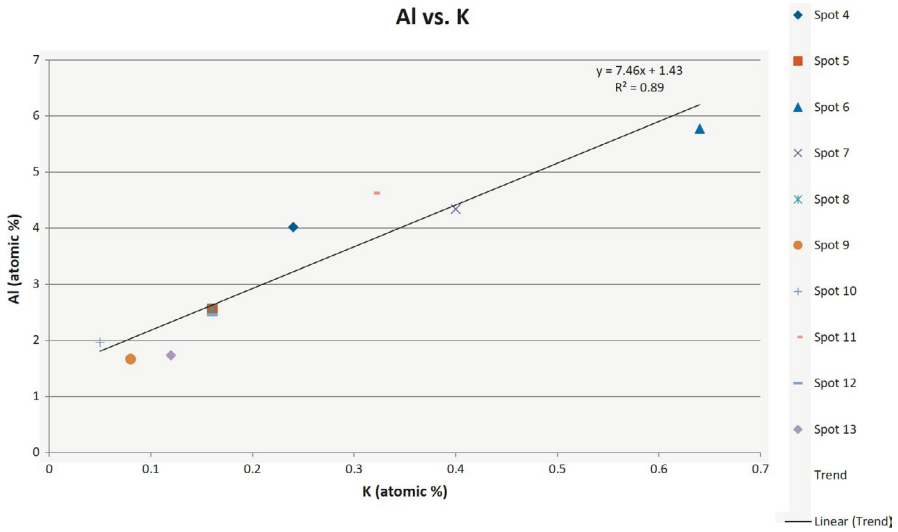

FIGURE 5 Plot of potassium versus aluminum concentrations measured by semi-quantitative EDS on the particle surface, showing a strong correlation (see Table1), r^2=.89

specifically, lead was not just on the particle surface but also within it.

Regarding the elements that were detected at very low atomic percent, it was perhaps most interesting to observe that chromium and iron were always detected together, specifically at sites 4, 6, 11, and 12. Curiously, these two transition metals were also detected with phosphorous at sites 4 and 12, but not at the third site of phosphorous detection, site 10. Finally, alkali metals and alkali earth metals were detected, present as magnesium in seven EDS sites, sodium in two EDS sites and calcium in two EDS sites, but always at low at %. In addition, chlorine was detected at five sites, also at low at %.

While the EDS data suggest that the purple pigment particle has a heterogeneous composition, there are some significant observations to summarize regarding them. With the exception of lead, the elements detected in the pigment are consistent with both plant-derived and insect-derived colorants. The co-detection of chromium with iron was a finding to highlight, and this might relate to a specifically selected mordant, intentionally or fortuitously, perhaps employed to adjust the ultimate color of an organic lake pigment. While there may be an association between phosphorous and insect-based colorants,[23] we detected only very small percentages of phosphorous; therefore, it seems unwise to suggest an insect-based colorant as opposed to a plant-based colorant on this basis.[24] The low sodium detected may suggest Egyptian natron was not used as an alkali in the preparation of this colorant.

2.2 | Atom probe tomography of the purple pigment particle

To explore the distribution of elements within the purple particle, atom probe tomography (APT) was conducted on three needles, milled from the purple particle using the focused ion beam (FIB) technique. Each needle was created with a volume of approximately 20 nm^3 for elemental characterization, one of which is shown in Figure 6. Historically, this technique has been used primarily to analyze metallic and semiconductor materials. With the advent a laser-assisted mode in state-of-the-art LEAP systems, it is now possible to characterize organic and insulating materials, such as ceramics, teeth, and bone.[26-28] To our knowledge, APT has not been performed on an organic pigment. Therefore, as noted above, a secondary purpose of presenting these data is to demonstrate that APT is a possible tool for examining organic pigments.

Atom probe tomography is a unique technique that provides information on the three-dimensional, spatial position of atoms and molecules, including light elements such as hydrogen, with near atomic resolution. In the case of the instrument used in these studies, the resolution is 0.5 Å along the z-axis and the detectable concentration can be as low as 1 ppm depending on the ion or molecule. It is therefore a way of sampling local chemistry and interfaces at a scale that is virtually nondestructive given the very small amount of

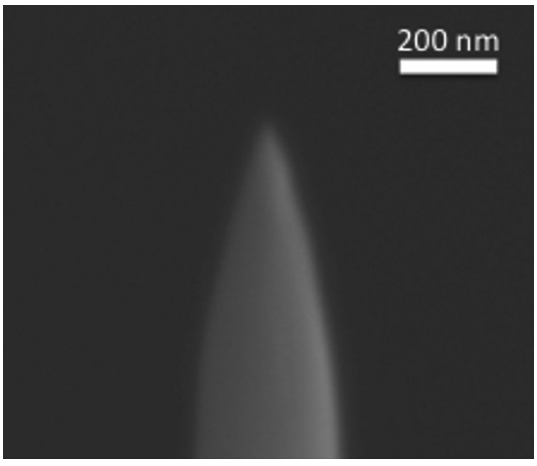

FIGURE 6 SEM image of one of three LEAP samples that were successfully extracted from the pigment particle by FIB

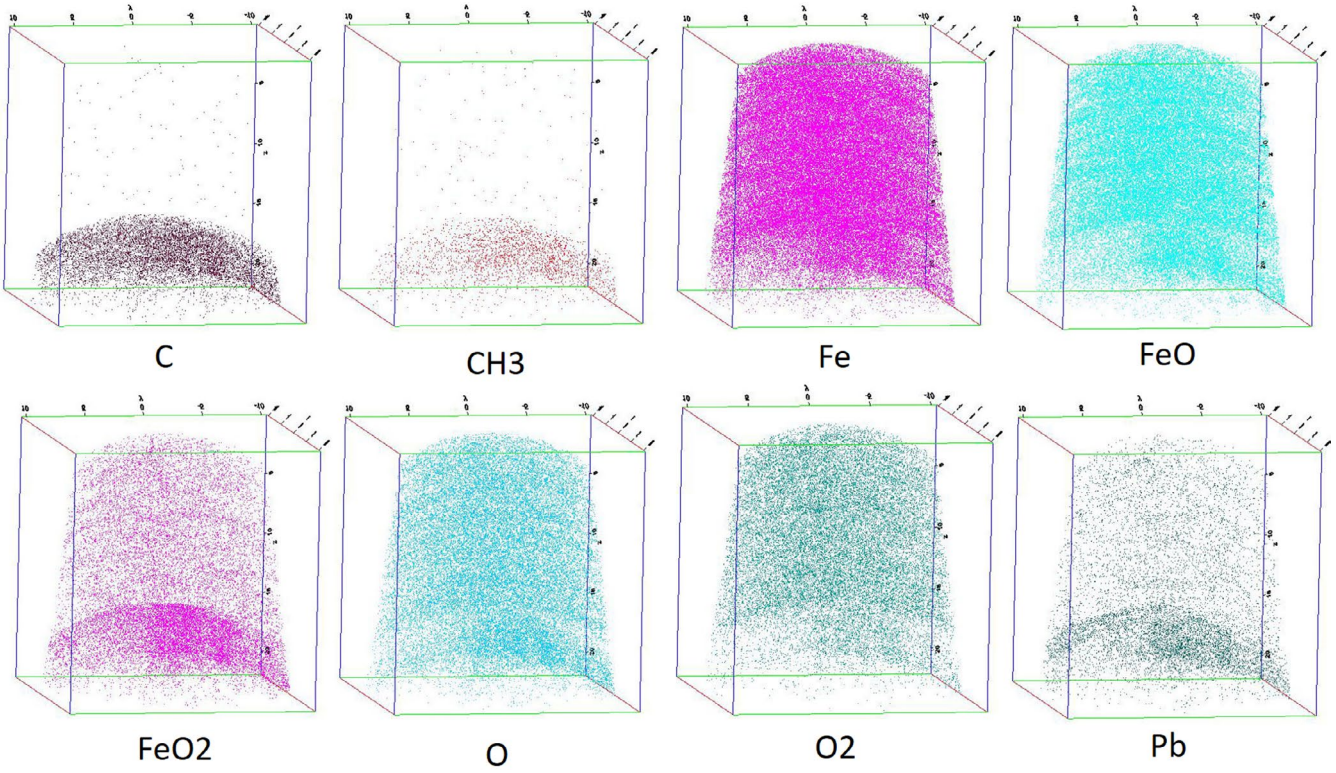

FIGURE 7 LEAP 3D elemental maps showing the distribution of C, H, O, Fe, and Pb in the specimen shown in Figure 7. Each box is 21 nm per side

material required to do the analysis, in this case an approximately 50 μm particle.

Attempts were made to characterize two of the APT samples using the conventional, voltage mode method of ionizing the material. This involves electrically energizing the tip of the needle by applying up to 11 kV, thus producing enough energy to sputter ions and charged molecules toward time-of-flight mass spectrometer and a position-sensitive detector. Although some chemical data were collected, these two attempts failed, as the tips appeared to fracture during the measurements due to the low electric and thermal conductivity of the pigment. Consequently, the third tip was analyzed using laser-assisted sputtering, successfully yielding the data shown in Figure 7.

This particular sample represents a very small volume, approximately 20 nm^3, and may not be representative of the entire material. Interestingly, LEAP results show a clear interface between two phases within the volume analyzed. The discovery of an interface within the particle was entirely unexpected because ancient lake pigments are understood to be amorphous.[24,25] The LEAP tip closer to the particle's exterior is richer in carbon and methyl [$-CH_3$] with lead and oxido(oxo)iron as FeO_2^-. More reduced iron seems to enrich the LEAP tip closer to the particle's interior region. Since the LEAP results were so surprising and difficult to interpret, given the randomly selected nanoscale volume analyzed and the detected interface, additional analyses were pursued using larger cross sections of the purple pigment particle and analyzed in transmission with diffraction to examine the broad chemistry of the pigment.

2.3 | Transmission electron microscopy of the pigment particle

To explore further the internal structure of the purple particle and understand better the distribution of elements within it, separate and distinct from interferences of the binding medium and admixed pigments in the surrounding paint, FIB was again employed to mill the roughly 100 μm^2 cross section of the particle shown in Figure 8. This FIB section was analyzed using transmission electron microscopy (TEM), focusing on seven regions of interest, ROI #1-7 indicated by red numbered circles in Figure 8, to examine the internal structure of the particle; diffraction was used to identify crystalline domains. Artifacts of the FIB process include a platinum protection layer that surrounds the FIB section, visible in Figure 8 as a bright white layer, and striations most visible on the bottom of the FIB section that can be considered milling marks from the focused ion beam. In the TEM-EDS data, gallium can be attributed to the ions used for the FIB, and most copper can be attributed to the copper grids used to support the sample during analyses.

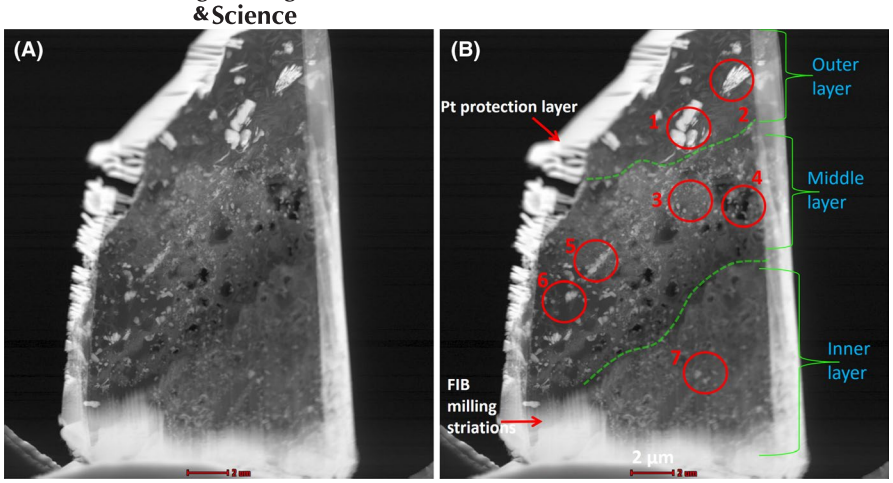

FIGURE 8 (A) STEM HAADF image of an extracted TEM sample on the left, showing heterogeneity and stratigraphy within the pigment; in (B) at right, annotations show regions of interest (ROI) marked #1-7 in red

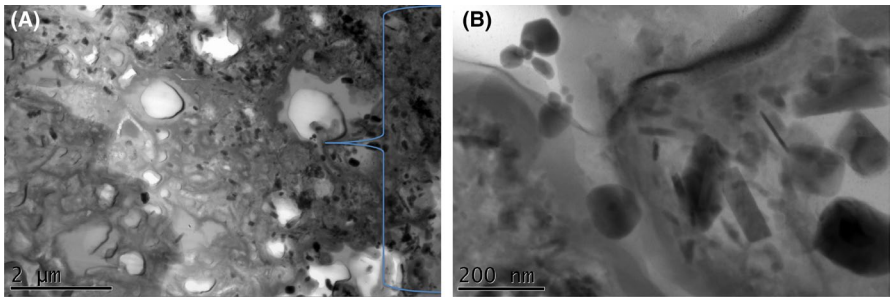

FIGURE 9 (A) TEM bright-field image taken at low magnification at left, showing a representative microstructure of the middle layer within the pigment, from ROI #1 in Figure 8, which is comprised of an amorphous, organic matrix, and nanometer scale crystallites; at right in (B) higher magnification is presented showing matrix, irregular/spherical particles, and needle-shaped particles

The FIB section in Figure 8 reveals crystalline inhomogeneities, and most surprisingly, stratigraphy within an ancient lake pigment—never reported previously to the authors' knowledge. Heretofore, lake pigments have been understood and described as amorphous.[24,25] It was surprising to observe within the lake pigment particle a variety of nanometer-scale particles that include irregular, spherical, and needle shapes that appear bright white, consistent with high-density material, clearly shown in Figure 9. Examination of the FIB section using optical microscopy, shown in Figure 10, revealed the expected bright red appearance consistent with anthraquinone-based colorants viewed under specific green illumination, a band pass 546/14 filter.

While X-ray EDS measurements detected the same elements as the SEM/EDS analyses previously described, the TEM/EDS analyses demonstrated much more effectively the level of compositional heterogeneity. In addition, TEM/EDS yielded another surprising observation: There are three clearly differentiated layers within the lake pigment particle. As distinguished by green dotted lines in Figure 8, there is an outer layer where large crystals evidence growth was favored over nucleation. In contrast, the inner layer is characterized by a multitude of small crystallites, suggesting nucleation was favored over crystal growth.

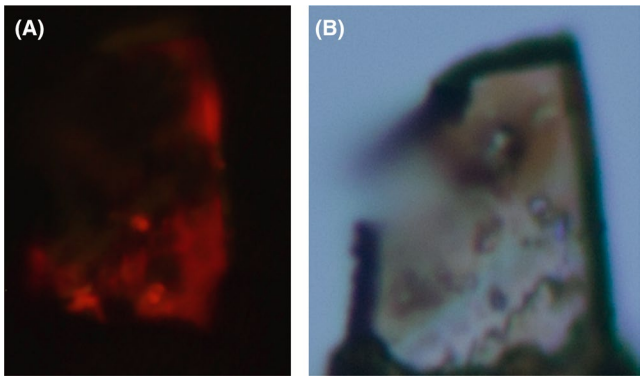

FIGURE 10 (A) At left is the sample imaged using light microscopy with the Leica-M2 (green) filter with Excitation: BP 546 nm/14, dichromatic mirror 580 nm, suppression filter LP590, showing the characteristic red response consistent with anthraquinone-based colorants. At right in (B) is the sample viewed under partially crossed polarizing filters, exhibiting some prior heat damage in the upper left following a characterization attempt with Fourier transform infrared spectroscopy

The outer layer is characterized by lead-based particles that are comparatively large—approximately 500 nm diameter; these particles appear bright white and some contain sulfur, with some also containing little calcium. These

lead-containing large particles are embedded in a matrix that appears dark, is rich in carbon with some oxygen, but sulfur and aluminum were not detected in the dark matrix. An EDS line scan of three crystallites in the outer layer is presented in Figure 11, from an area within ROI#1.

The interior of the pigment can be loosely described as comprised of nanometer-scale crystallites that appear bright white, within an amorphous, organic matrix that appears dark; diffraction yielded no results from the dark areas of the matrix. Presumably, both the matrix and the particles contribute to the overall color of the pigment. In general, the interior matrix was found to be very rich in carbon and oxygen, deplete of most other elements, but always with minor concentrations of sulfur, aluminum, and lead. Fewer crystallites were observed in the inner layer, and these were smaller with <100 nm diameter.

The middle layer of the pigment particle is presented in Figure 12, from ROI#5. The composition of the particles varied considerably, but they were generally rich in either lead or aluminum or both. Outside the brightest, lead-rich areas, the other metal elements described above were also detected in minor and varying amounts. Chromium was only detected with certainty in the middle layer, and when chromium was detected, it was always with iron and phosphorous. Most of the sulfur and oxygen was associated with the crystallites rather than the matrix. In general, lead was the predominant

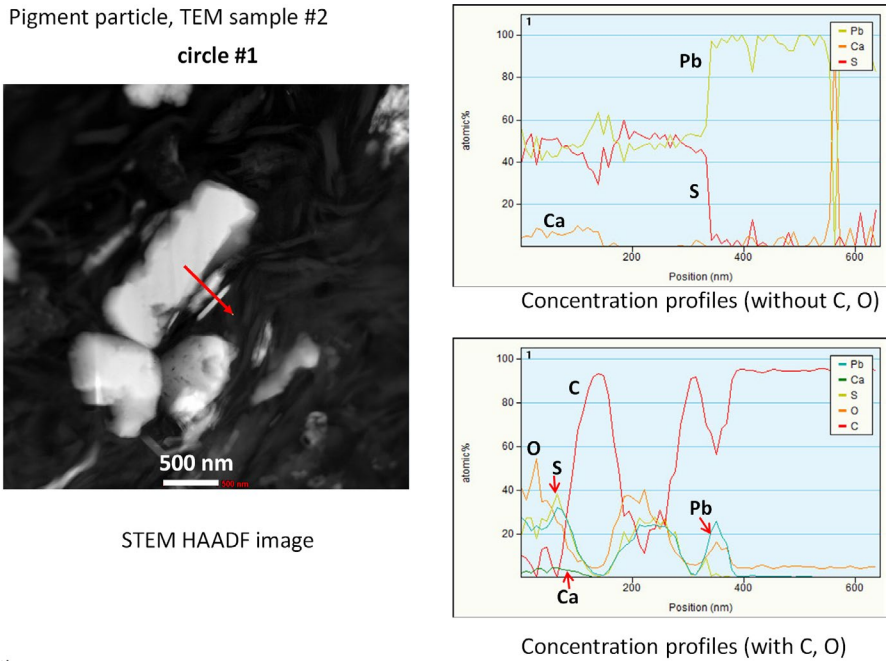

FIGURE 11 Elemental data derived from a line scan of three crystallites in the outer layer, from ROI #1 in Figure 8

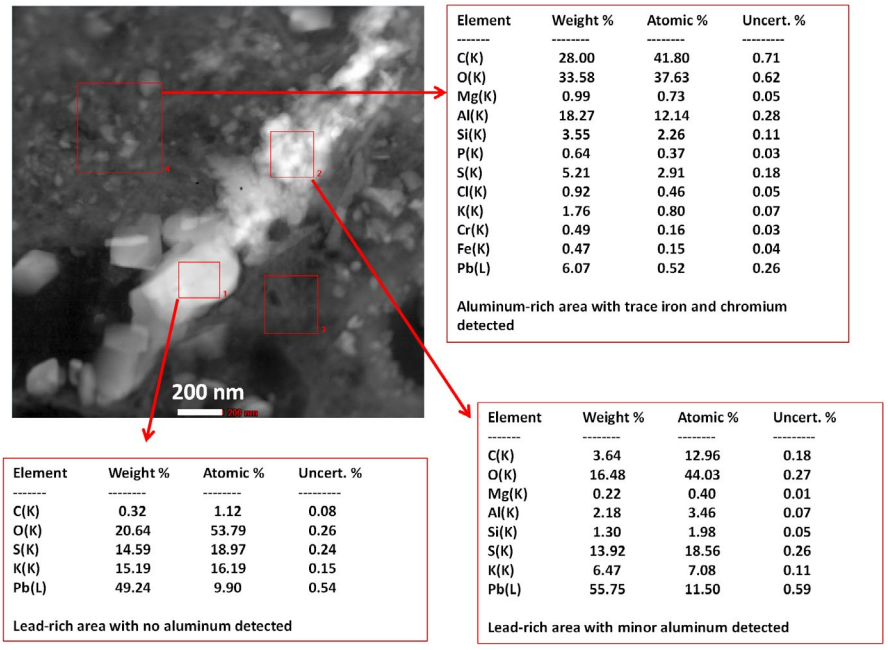

FIGURE 12 The middle layer from ROI #5 in Figure 8 showing the presence of chromium with iron, and lead-rich areas with aluminum and without aluminum

metal component of the majority of particles in the middle layer, characterized by numerous crystallites that were <200 nm diameter.

2.4 | Diffraction and crystallite identification

Six of the larger, bright, lead-containing particles were characterized by diffraction to determine the phase of the crystallites. We were able to identify only two common crystalline phases among those particles that we were able to analyze, orthorhombic (Pnma) $PbSO_4$ and $PbCO_3$. Figures 13 and 14 show a TEM image and diffraction patterns, respectively, for a representative, $PbSO_4$ particle from the middle layer of the pigment particle. In order to determine the crystal structure of a grain, a minimum of three electron diffraction patterns (EDPs) must be obtained at different tilt angles. Figure 14 shows EDPs obtained at three tilt angles form the grain shown in Figure 13. Based on the zone axes and directions between the EDPs, and the measured d-spacings and angles between the indexed planes in each EDP, combined with the EDS chemical analyses, this specific particle was found to have a structure and composition consistent with orthorhombic, Pnma (S.G. 62)[29] $PbSO_4$. For comparison to the EDPs, simulated patterns for this structure are also shown in Figure 14. The simulations were done using CaRIne crystallography software (Cyrille Boudias and Daniel, Monceau, France) based on the data for $PbSO_4$ from Pearson Crystal Data.[29] Figures 15 and 16 show a second TEM image and diffraction patterns, respectively, for a representative, orthorhombic, Pnma (S.G. 62)[29] $PbCO_3$ particle from the outer layer of the pigment particle. A large number of particles with similar morphology and contrast were analyzed with EDS, and all were generally comprised of Pb, O, C, and/or S and often minor amounts of either Al or Ca.

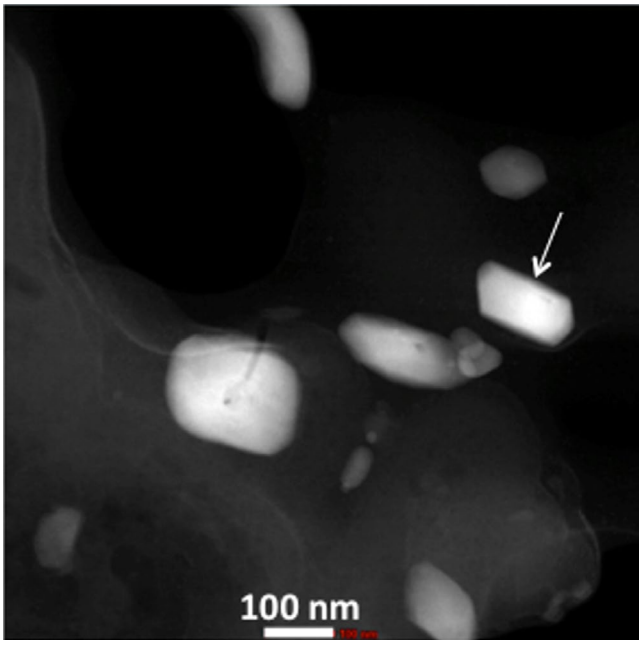

FIGURE 13 STEM HAADF (high-angle annular dark field) image of several crystallites observed in the pigment matrix that was comprised of lead, oxygen, sulfur, and carbon, with a minor percentage of aluminum. The arrow denotes the grain from which the diffraction data in Figure 14 were obtained. The particle was determined to have a crystal structure consistent with that of orthorhombic $PbSO_4$, Pnma[29]

2.5 | An ancient dyers workshop connection

All of these reported findings point to a close association between the purple pigment particle and ancient dye practice and technology. The nanometer scale and the facetted morphology suggest that the lead carbonate and lead sulfate crystals nucleated and grew as the pigment particle formed. The lead carbonates and lead sulfates are much too small to be explained as artists' materials added intentionally or unintentionally as white pigment. It is much more reasonable to suggest that the source of the lead is a material, such as a crucible, used during production of the pigment. We speculate that the lead source is a lead-lined dyeing vat akin to that described by Flinders Petrie for his classic 1908 excavations of the Ptolemaic Egyptian dyers workshop of Athribis.[30] Moreover, the fact that the lead-containing crystallites within the pigment particle contain varying concentrations of sulfur and carbon suggests the crystallites derive from more than one source; specifically, the lead additions may not have been intentional or by design.

Furthermore, the diffraction results for the six lead-containing crystallites interestingly divide between lead carbonates identified in the outer layer, but in the middle layer, lead sulfate is identified, with chromium and iron; the inner layer produced no diffraction data. This stratigraphy observed in the purple pigment particle corresponds to the steps of the so-called "development" dyeing process. First, fabric is soaked/simmered in an alum or potassium aluminum sulfate solution as a premordanting step, and then, it is washed and placed in the dye bath to simmer. These steps can be combined in one-bath dyeing; in either case, the process is consistent with the high nucleation rate and small crystallites observed in the inner layer of the pigment particle. Next, metal salts are added producing the colored lakes characteristic of the development dyeing process.[31] This is consistent with the moderately sized lead sulfate crystallites and the iron with chromium detected in the middle layer of the pigment particle. Development dyeing is addressed in the Stockholm-Leyden papyrus describing mordanting and dyeing fast purple: "if you wish the purple to be dark, add a little chalcanthus," or *chalkanthos*, copper and iron sulfates.[32] The presence of comparatively large lead carbonates in the outer layer suggests a period of

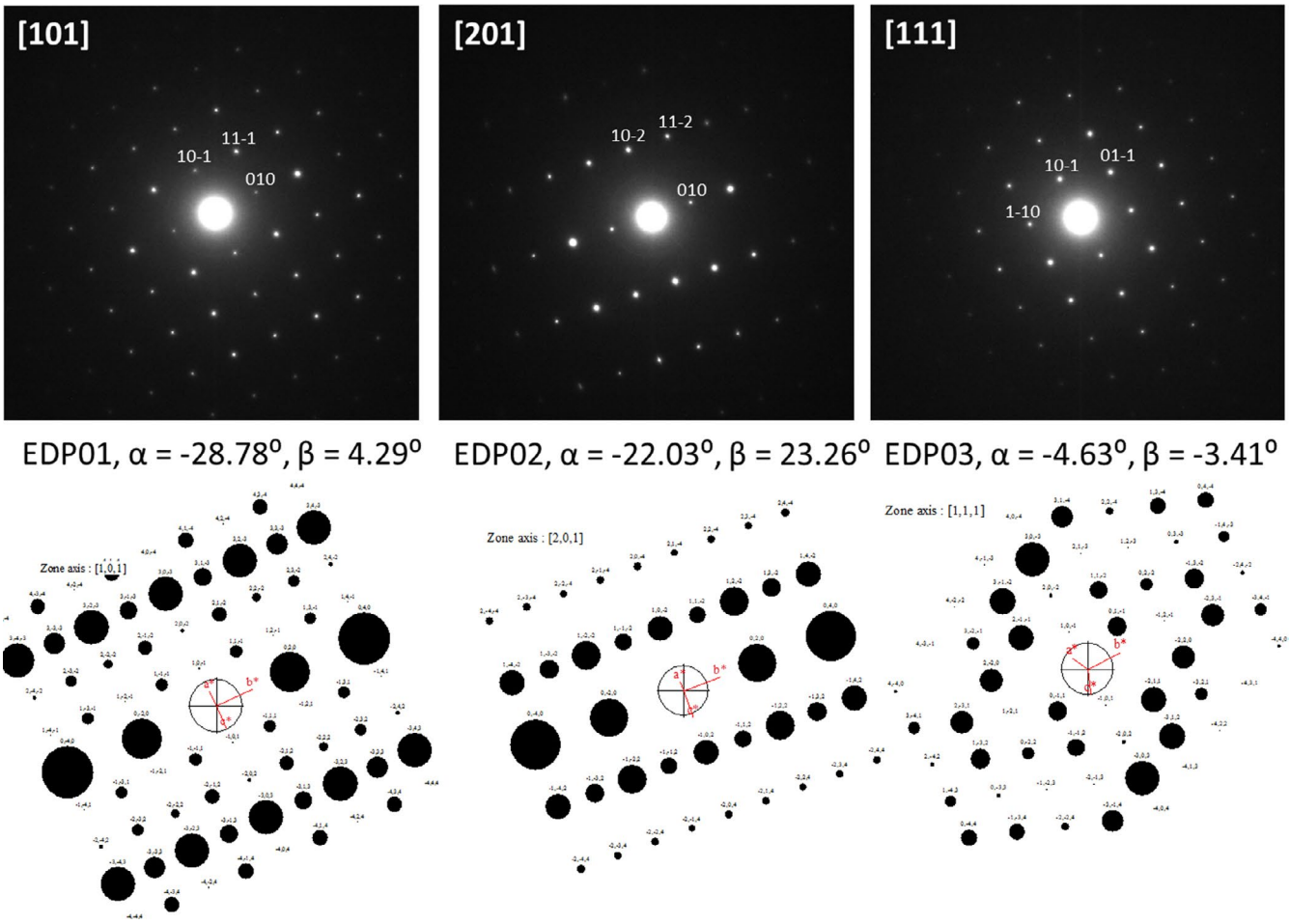

FIGURE 14 Electron diffraction patterns obtained on three orientations ([101], [201], and [111]) from the crystallite shown in Figure 13 and three simulated patterns matching those of the $PbSO_4$, Pnma (62), and orthorhombic structure[29]

digestion in an alkaline environment, such as that of the dye bath, where alkaline solution is used for dye extraction and stabilization.[24,25]

Therefore, we propose that the purple pigment particle is actually recycled, or more appropriately, upcycled dye sludge, specifically the particulate residues remaining at the bottom of an ancient dye vat—solids recovered and repurposed to paint the mummy portrait, exemplifying resource maximization in Roman Egypt. Such upcycling may explain the presence of fibers in the purple and pink paints observed in some mummy portraits, as shown in Figure 17. Similar recycling or upcycling in the Roman era was reported on "red-shroud mummies" where the red minium pigment, Pb_3O_4, was generated from the lead oxides associated with silver cupellation at the Rio Tinto site in modern Spain.[33]

3 | CONCLUSIONS

Analysis of an approximately 50 μm particle of purple pigment from the clavi depicted in the Mummy Portrait of a Bearded Man, painted around 170-180 CE, was carried out by a combination of SEM/EDS, STEM/EDS/diffraction, and APT-LEAP. Analyses demonstrated that the particle was a heterogeneous organic pigment, containing minor percentages of transition metals and alkali / alkali earth metals, with nanometer-scale crystallites of lead-aluminum rich carbonates and sulfates. A stratified structure of the particle was observed in the particle's cross section; this is the first time a microstructure is reported within a lake pigment. Strata were differentiated by crystallite size, with smaller, interior crystallites <200nm diameter suggesting nucleation processes were favored, and with larger, exterior crystallites, *circa* 500nm diameter, suggesting crystal growth. In addition, lead carbonate crystallites were detected in the outer strata, and lead sulfates were detected in the middle strata with chromium and iron. No crystallographic data were obtained for the organic-rich regions throughout the pigment particle, confirming previous descriptions of such as amorphous.[24]

As can be the case with analytical studies of cultural heritage materials, particularly so with museum objects, we present substantiated conjecture based on our findings, but without certainty of scientific proof. The composition and

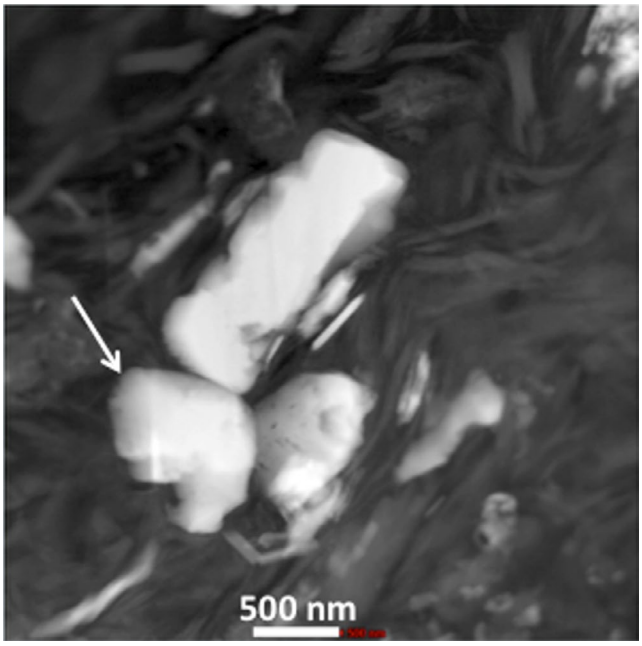

FIGURE 15 STEM HAADF image of several crystallites observed in the pigment matrix that was comprised of lead, oxygen, and carbon, with a minor percentage of calcium. The arrow denotes the grain from which the diffraction data in Figure 16 were obtained. The particle was determined to have a crystal structure consistent with that of orthorhombic $PbCO_3$, Pnma[29]

microstructure suggest that the purple pigment was synthesized in a leaded container, using a dye derived from insect or plant matter. The question of intentional or unintentional utilization of chromium remains unresolved: Chromium could reasonably be expected to be an impurity in an iron source or an impurity in an alum source; as pink alum was exploited as an ancient Egyptian cobalt source for producing blue glass in imitation of lapis lazuli.[34] Whether a chromium-rich ingredient was preferentially utilized remains a question.

This research does, however, provide an association of the Walters *Portrait of a Man* to another unprovenienced mummy portrait. Of all the institutions participating in the APPEAR analyses of mummy portraits, only the MFA-Houston reports the detection of chromium in the purple paint in one mummy portrait, TR-184-2013, a *Portrait of a Young Girl*, see Figure 18. While the two portraits have apparently not been stylistically related previously, the two portraits do certainly have physical similarities, specifically, the panel shape and the background tone. Additionally, both portraits share stylistic similarities that include the turn of the neck and the direction of the eyes. The rendering of hair, eyebrows, eyelashes, and clothing are visual characteristics of both the Walters and MFAH portraits that are also shared with provenienced mummy portraits from the general Faiyum region that includes Darb Gerze (Philadelphia), Er-Rubayat, and El-Hibeh (Ankyronpolis).[35] While it remains to be determined how many mummy portraits have similar chromium-containing purple paint, these findings do suggest that transition metal-mordant similarities may be useful to help associate unprovenienced mummy portraits to similar time and place of production.

4 | EXPERIMENTAL PROCEDURES

Because of the portrait's importance and fragile condition, permission was granted from the Walters Museum to extract a single, small particle of pigment from the encaustic wax paint binder, an example of which is visible in Figure 3A. Specifically, using a deft scalpel, an approximately 50 μm sample was carefully separated from the wax media and was then sandwiched between two glass slides, one having a convex recess to retain the particle. The particle was analyzed through a polyester envelope at the Walters Art Museum using the air-path ARTAX X-ray Fluorescence spectrometer equipped with a micro focus 80-μm polycapillary lens, powered at 50kV and 700 μAmp for 300 sec acquisition time with a helium purge. Following optical characterization at the Walters Art Museum, the particle was shipped to Boise State University for characterization.

The particle, shown in Figure 3B, was carefully transferred from the glass slide under an optical microscope (KEYENCE Corp., VHX-S50) at 100x magnification to a double-sided carbon tape mounted on a scanning electron microscope (SEM) sample stub. The transfer was done by first lightly touching a superfine eyelash (Ted Pella, Inc.) to the adhesive of the carbon tape, thereby transferring some adhesive to the eyelash. The particle was then touched lightly with the eyelash, adhered, and was transferred and affixed to the carbon tape.

Scanning electron microscopy and energy-dispersive X-ray spectroscopy (EDS) were carried out using a JEOL JSM-6610LV (JEOL USA, Inc.) in order to characterize the morphology and local chemistry of the particle and to identify candidate areas for ion milling of samples for transmission electron microscopy (TEM) and atom probe tomography (APT). Two TEM lamella and three APT samples were removed from regions of the particle as shown in Figure 4A using a lift-out technique in a focused ion beam (FIB) (FEI Quanta 3D FEG). Figure 4B shows an image of the pigment particle following lift-out of several TEM and APT samples. Conventional TEM and scanning TEM (STEM) were done using a Tecnai G^2 F30 STEM FEG (FEI). Atom probe tomography was done using a LEAP 4000X HR 3-dimensional local electrode atom probe (CAMECA) in both laser mode (40-60 pJ energy, 100 kHz pulse rate, 30-50 K tip temperature, in a 3×10^{-11} torr vacuum) and voltage mode (50 K tip temperature, 100 kHz pulse rate, 20% pulse fraction). The chemical identity of each charged particle was analyzed during LEAP by time-of-flight mass spectroscopy. The APT data analyses

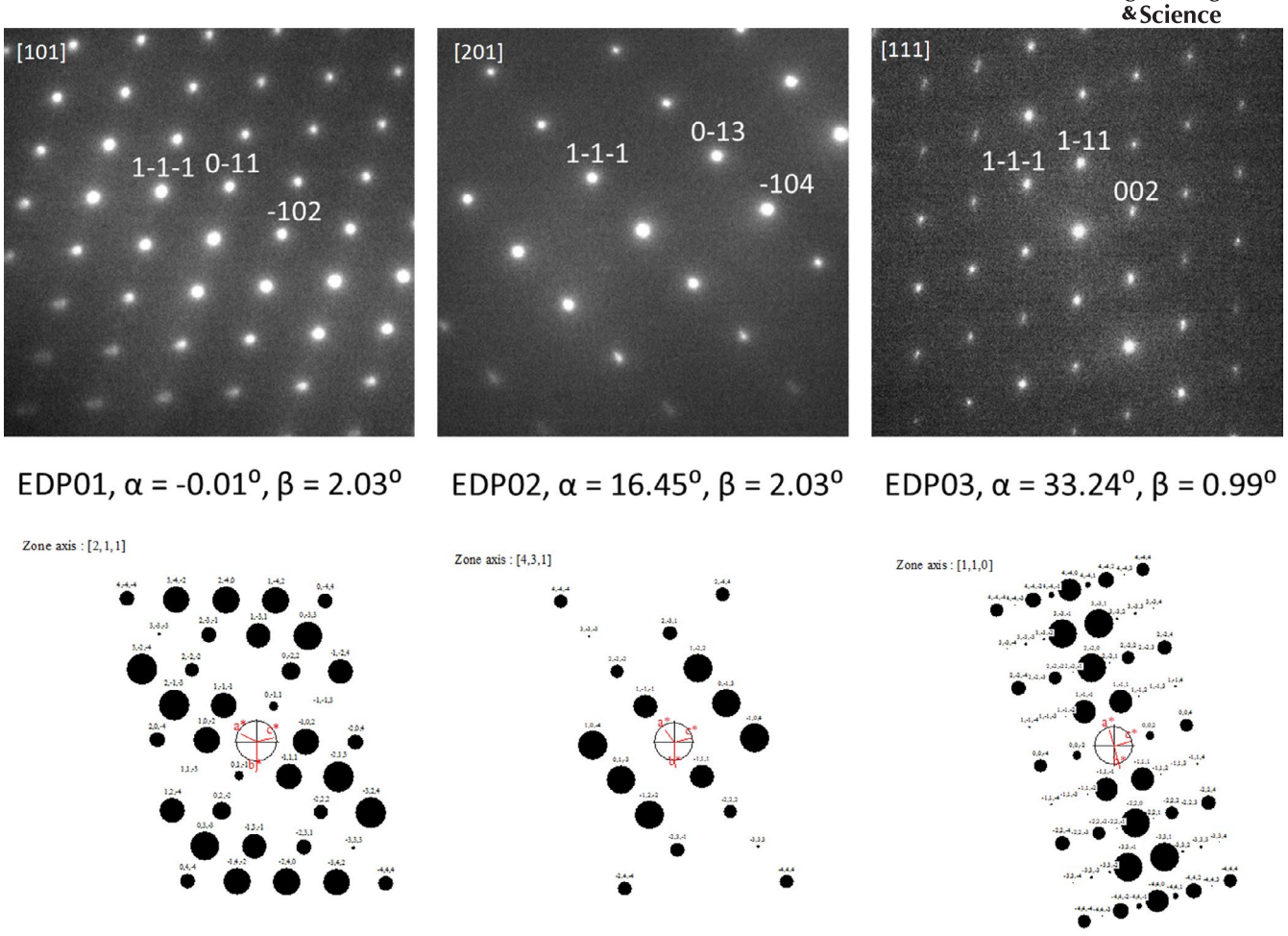

FIGURE 16 Electron diffraction patterns obtained on three orientations ([101], [201], and [111]) from the crystallite shown in Figure 15 and three simulated patterns matching those of the $PbCO_3$, Pnma, and orthorhombic structure[29]

FIGURE 17 Fibers observed in the paint used for a mummy portrait; detail of *Mummy Portrait of a Woman in Pink Tunic* 79.AP.129 J. Paul Getty Museum

and 3D reconstruction were done using CAMECA IVAS software. It should be noted that to our knowledge these are the first TEM and APT studies of an ancient organic pigment. Thus, the FIB, TEM, and APT methods were performed not only to characterize the microstructure and chemistry of the pigment, but to demonstrate the feasibility of using these relatively new techniques for what may best be described as effectively nondestructive due to the microscopic scale of damage left in the artifact.

ACKNOWLEDGMENTS

The authors are grateful for many enlightening discussions with staff at the Walters Art Museum and undergraduate and graduate students in D. Butt's research group and materials art courses, including Brittany Cannon, Jared Talley, Alaggio Laurino, Cameron Quade, John Paul Stroud, Brittany Archuleta, Ron Garnys, Brian Jaques, Gordon Alanko, and Brian Jaques. This work was partially funding by the Boise State University Office of Research and the College of Innovation and Design as part of a Vertically Integrated Research Program. Special thanks to Drs. Mark Rudin, Harold Blackman, William Hughes, and Sian Mooney for their support and enabling of this activity. All authors are indebted to the Center for Advanced Energy Studies - Microscopy and Characterization Suite in Idaho Falls, ID for much analyses

FIGURE 18 Museum of Fine Art—Houston, TR-184-2013, a *Portrait of a Young Girl* with chromium detected in the purple paint

and assistance. At the Walters, thanks to Lisa M. Anderson-Zhu, Associate Curator, Art of the Mediterranean, 5th millennium BCE to 4th century CE, and Julie Lauffenburger, Dorothy Wagner Wallis Director of Conservation, Collections and Technical Research, and Elizabeth LaDuc and Geneva Griswold for contributions during their internships; with special thanks to the Andrew W. Mellon Foundation for financial support of conservation science. The authors are indebted to Corina E. Rogge, The Museum of Fine Arts Houston and the Menil Collection, for research assistance and review; Barbara Berrie for much technical assistance; and Marie Svoboda for all her assistance with mummy portrait studies.

ORCID

Glenn Gates https://orcid.org/0000-0002-5913-7074
Yaqiao Wu https://orcid.org/0000-0002-5041-0935
Jatuporn Burns https://orcid.org/0000-0001-5654-9957
Jennifer Watkins https://orcid.org/0000-0003-3673-5618

REFERENCES

1. Pliny BJ, Riley H. The Natural History of Pliny. London: H. G. Bohn; 1855.
2. Thompson D. Mummy portraits in the J. Paul Getty Museum. Malibu: The J. Paul Getty Museum; 1982.
3. Corcoran L, Svoboda M. Herakleides: A Portrait Mummy from Roman Egypt. Los Angeles: Getty Publications; 2010.
4. Montserrat D. The representation of young males in 'Faiyum Portraits'. J Egypt Archaeol. 1993;79:215–225.
5. Borg B, Most G. The Face of the Elite. Arion. 2000;8(1):63–96.
6. The seven original APPEAR institutions include: The J. Paul Getty Museum, British Museum, Walters Art Museum, Ny Carlsberg Glypotek, Phoebe Hearst Museum of Anthropology, Ashmolean Museum of Art and Archaeology, and the Museum of Fine Arts, Boston. As of 2020, forty eight institutions are participating. For details on the project, see: http://www.getty.edu/museum/research/appear_project/.
7. Bender Jørgensen L.Clavi and non-clavi: definitions of various bands on roman textiles. Purpureae Vestes III. Textiles y Tintes en la ciudad antiqua. Actas del III Symposium Internacional sobre Textiles y Tintes del Mediterráneo en el mundo antiguo (Naples 2008). 2011. p. 75–81.
8. Cartwright C, Spaabaek LR, Svoboda M. Portrait mummies from Roman Egypt: Ongoing collaborative research on wood identification. Br Museum Tech Res Bull. 2011;5:54–56.
9. Finley V. Color, A Natural History of the Palette. New York: Random House; 2002.
10. Clark R, Cooksey C, Daniels M, et al. Indigo, woad, and Tyrian purple: important vat dyes from antiquity to the present". Endeavour. 1993;17(4):191–199.
11. Reinhold M. History of purple as a status symbol in antiquity. Collection Latomus 116. Brussels: Latomus, Revue d'Études Latines. 1970.
12. Abdel-Kareem O. History of dyes used in different historical periods of Egypt. Res J Textiles and Apparel. 2012;16(4):79–92.
13. Schatz P. Indigo and Tyrian purple – in nature and in the lab. J Chem Ed. 2001;78(11):1442–1443.
14. Aceto M, Arrais A, Marsano F, et al. A diagnostic study on folium and orchil dyes with non-invasive and micro-destructive methods. Spectrochim Acta Part A Mol Biomol Spectrosc. 2015;142:159–168.
15. Morales K, Berrie B.A note on characterization of the cochineal dyestuff on wool using microspectrophotometry. E-Preservation Science [serial online]. 2015 [cited 2020 Oct 19];12:8–14.
16. Barber E. Prehistoric Textiles: The Development of Cloth in the Neolithic and Bronze Ages with Special Reference to the Aegean. Princeton: Princeton University Press; 1992.
17. Reardon A. Metallurgy for the Non-Metallurgist, 2nd edn. Materials Park: ASM International; 2011.
18. Tobia S, Sayre E. An analytical comparison of various Egyptian soils, clays, shales and some ancient pottery by neutron activation analysis. In: Bishay A, ed. Recent Advances in Science and Technology of Materials. New York: Plenum; 1974:99–128.
19. Ferreira E, Hulme A, McNab H, et al. The natural constituents of historical dyes. Chem Soc Rev. 2004;33:329–336.
20. Salzberg H. From Caveman to Chemist: Circumstances and Achievements Washington. Am Chem Soc. 1991.
21. Brunello F. The Art of Dyeing in the History of Mankind. Vicenza: Neri Pozza; 1973.
22. Picon M, Vichy M, Ballet P.Alum western oasis of Egypt: field research and laboratory research. In: Borgard P, Brun JP, Picon M, editors. Alum Mediterranean [serial online]. 2005 [cited September 14, 2016]; 43–57.
23. Nevin A, Osticoli I, Comelli D, et al.Advances in the analysis of red lake pigments from 15th and 16th C. paintings using fluorescence and Raman spectroscopy. Paper presented at: Art'11 10th International Conference on the non-destructive investigations and

microanalysis for the diagnostics and conservation of cultural and environmental heritage, 2011 April 13–15; Florence, Italy [serial is on CD-ROM and online, six pages, cited 2016 Sept 14].
24. Kirby J, Spring M, Higgitt C. The technology of red lake pigment manufacture: study of the dyestuff substrate. Nat Gal Tech Bull. 2005;26:71–86.
25. Clementi C, Doherty B, Gentili P, et al. Vibrational and electronic properties of painting lakes. Appl Phys A. 2008;92(1):25–33.
26. Gordon L, Joester D. Nanoscale chemical tomography of buried organic-inorganic interfaces in the chiton tooth. Nature. 2011;469:194–197.
27. Gordon L, Tran L, Joester D. Atom probe tomography of apatites and bone-type mineralized tissues. ACS Nano. 2012;6:10667–10675.
28. Gordon L, Cohen M, MacRenaris K. Amorphous intergranular phases control the properties of rodent tooth enamel. , et al. Science. 2015;347:746–750.
29. Pearson's Crystal Data. Crystal structure database for inorganic compounds release 2011/12, ASM International, Materials Park, OH.
30. Petrie F. Anthribis. London: School of Archaeology University College; 1908.
31. Schweppe H. Practical Hints on Dyeing with Natural Dyes. Washington: Smithsonian Institution; 1986.
32. Singer C. The Earliest Chemical Industry. London: The Folio Society; 1948.
33. Walton M, Trentelman K. Romano-Egyptian red lead pigment: a subsidiary commodity of Spanish silver mining and refinement. Archaeometry. 2009;51(5):845–860.
34. Shortland A, Tite M, Ewart I. Ancient exploitation and use of cobalt alums from the western oases of Egypt. Archaeometry. 2006;48:153–168.
35. The authors are indebted to Lisa M. Anderson-Zhu for this visual analysis.

How to cite this article: Gates G, Wu Y, Burns J, Watkins J, Butt DP. Microstructural and chemical characterization of a purple pigment from a Faiyum mummy portrait. *Int J Ceramic Eng Sci*. 2021;3:4–17. https://doi.org/10.1002/ces2.10075